NJC

Accepted Manuscript

This is an *Accepted Manuscript*, which has been through the Royal Society of Chemistry peer review process and has been accepted for publication.

Accepted Manuscripts are published online shortly after acceptance, before technical editing, formatting and proof reading. Using this free service, authors can make their results available to the community, in citable form, before we publish the edited article. We will replace this *Accepted Manuscript* with the edited and formatted *Advance Article* as soon as it is available.

You can find more information about *Accepted Manuscripts* in the Information for Authors.

Please note that technical editing may introduce minor changes to the text and/or graphics, which may alter content. The journal's standard Terms & Conditions and the Ethical guidelines still apply. In no event shall the Royal Society of Chemistry be held responsible for any errors or omissions in this *Accepted Manuscript* or any consequences arising from the use of any information it contains.

ROYAL SOCIETY OF CHEMISTRY

www.rsc.org/njc

Cite this: DOI: 10.1039/c0xx00000x

www.rsc.org/xxxxxx

ARTICLE TYPE

Controllable synthesis of spherical anatase mesocrystals for lithium ion batteries

Xinxin Fu, Binbin Wang, Chao Chen, Zhimin Ren, Chenyao Fan and Zhiyu Wang*[a]

Received (in XXX, XXX) Xth XXXXXXXXX 20XX, Accepted Xth XXXXXXXXX 20XX

DOI: 10.1039/b000000x

In this article, spherical anatase mesocrystals have been successfully prepared in acetic acid-tetrabutyl titanate-benzoic acid system *via* a facile solvothermal method. Based on the results of time-dependent experiments, the growth process of spherical mesocrystals was proposed, which involved formation of flower-like intermediates, hydrolysis of intermediates, precipitation and self-assembly of TiO_2 nanocrystals. During the formation procedure of spherical morphology, benzoic acid plays a very important role. Well-defined spherical anatase mesocrystals can be obtained only when benzoic acid content is more than 4.5 g. Owing to their unique architecture, which possesses high crystallinity and large specific surface area simultaneously, the lithium ion storage capabilities of these spherical mesocrystals were also investigated. The first discharge capacity is 314.5 mAh/g and the corresponding charge capacity is 224.3 mAh/g, leading to the Coulombic efficiency of 71.3% at 0.2 C. Even if under high current density, such as 2 C and 5 C, this anode material remains good cycling stability and very high specific capacity.

Introduction

Recently, hierarchical structures have attracted extensive attention for their outstanding properties and promising applications in environmental and energy areas.[1-3] Hierarchically mesoporous TiO_2 shows higher photocatalytic activity than P25 for the enhanced light-harvesting ability.[4] In addition, hierarchically porous $Li_4Ti_5O_{12}$ microspheres exhibit ultrahigh capability and excellent capacity retention over 200 cycles at high rates.[5] Generally, hierarchical structures are polycrystalline and constructed by low-dimensional (0D, 1D, 2D) building blocks. However, as a unique hierarchical architecture, mesocrystals always present a single-crystal-like atom structure for their nanosubunits sharing the same crystallographic orientation, and have received rapidly increased attention since they were proposed as a new class of ordered nanoparticle superstructures by CÖlfen and Antonietti for the first time in 2005.[6] They are considered as kinetically metastable species or intermediates in a crystallization reaction.[7-9] In sharp contrast to classical atom/ion/molecule-based mechanism, the growth of mesocrystals may involve a nonclassical, self-assembly-based crystallization process.[6] According to the information above, it can be concluded that mesocrystals can possess large specific surface areas and high crystallinity simultaneously. Therefore, scientists insights gradually turned to the synthesis of mesocrystals and their applications in fields like lithium ion battery, photocatalysis, *etc*.[10-12]

Up to now, various kinds of metal oxide mesocrystals such as ZnO,[13] CeO_2,[14] Fe_2O_3[15] and TiO_2[16-21] have been successfully synthesized. Titanium oxide (TiO_2), as an important functional metal oxide material, has achieved additional concerns owing to its excellent physicochemical properties and wide applications in various areas.[22-24] Many works on the preparation of TiO_2 mesocrystals have been reported recently. Zhou *et al.* firstly synthesized anatase TiO_2 mesocrystals *via* a topological conversion using NH_4TiOF_3 mesocrystals as precursors and studied their growth mechanism.[16] Furthermore, they also systematically investigated the influences of different experimental parameters such as surfactants, reaction temperature and stirring time on the anatase mesocrystals.[17] Since then, researches on the synthesis of mesocrystal TiO_2 sprung up, but very few about morphology controllable preparation.[18-21] As known to all, the usage of surfactant will be an effective way to realize the anisotropic growth of nanocrystals, thus shaping an ideal structure.[25] Therefore, based on the previous results, we attempt to introduce appropriate surfactants in the reaction system, thereby realizing the controllable preparation of TiO_2 mesocrystals.

TiO_2 is also one of potential anode materials for lithium ion batteries due to its high working voltage (1.78 V *vs* Li) and structural stability during lithium insertion/extraction processes.[19, 26-28] The electrochemical properties of TiO_2 are strongly depended on the diffusion distance of Li^+, electrical conductivity, particle size, morphology and architecture.[29-32] It is well known that spherical morphology is the optimal morphology in electrode fabrication art for the high packing density and good particle mobility.[33, 34] In this regard, spherical anatase mesocrystals may have outstanding performances in lithium ion batteries. Unfortunately, there are few papers on the synthesis of spherical anatase mesocrystals till now.[21]

Hence, in this article, we report a controllable synthesis of spherical anatase mesocrystals using benzoic acid as surfactant. Some contrast experiments were performed to explore the role of benzoic acid in controlling the morphology of anatase mesocrystals. Furthermore, we also evaluated their potential applications in the lithium ion batteries. When used as anode materials, they present pretty good cycling stability and rate performances, and will be promising electrode materials in the near future.

Experimental

Synthesis of spherical anatase mesocrystals

All the reagents were purchased from Shanghai Chemical Reagent Co. and used without further purification. Spherical anatase mesocrystals were prepared *via* a solvothermal method in the acetic acid (HAc) solution, using benzoic acid (BA) as surfactant, tetrabutyl titanate (TBT) as titanium precursor.

In a typical synthesis, 4.5 g BA was added into 30 mL HAc under vigorous stirring. After dissolved sufficiently, 0.75 mL TBT was added into the solution. The resulting suspension was transferred into a Teflon autoclave with a capacity of 75 mL and further stirred for one hour at room temperature. The vessel was then sealed, heated up to 200 ℃ and maintained for 24 h. After cooling down to room temperature naturally, the white precipitate was harvested *via* centrifugation, washed thoroughly with ethanol and deionized water for several times. Subsequently, these products were dried at 70 ℃ overnight. In order to remove the residual organics, the white powder was calcined at 400 ℃ for 30 min and spherical anatase mesocrystals were finally obtained. Series of time-dependent experiments were conducted to investigate the growth mechanism, as well as various benzoic acid additions were introduced to explore its role in controlling the shape of TiO_2 mesocrystals.

Characterization

The crystal structure and morphology of obtained products were characterized by powder X-ray diffraction (XRD, Philips PW1050, Cu Kα), field emission scanning electron microscopy (FESEM, Hitachi S4800, 5 kV), transmission electron microscopy (TEM, JEM-1230, 80 kV) and high-resolution TEM (HRTEM, Hitachi H-9500, 300 kV). Micromeritics TriStar 3020 instrument was performed to measure the nitrogen adsorption-desorption isotherm of spherical anatase mesocrystals and the surface area was calculated by multipoint Brunauer-Emmett-Teller (BET) method using the adsorption data in the range of P/P_0 from 0.1 to 0.30. The pore size distributions of the samples were derived from the desorption data using the Barett-Joyner-Halenda (BJH) model.

Electrochemical measurement

The electrode was prepared by mixing active materials (80 wt.%), acetylene black (10 wt.%), and polyvinylidene fluoride (10 wt.% PVDF) in N-methylpyrrolidone (NMP) into a homogenous slurry. The slurry was then spread onto copper foils and dried at 120 ℃ overnight in a vacuum oven. The average mass loading of the prepared electrodes is 1.0 mg. The electrochemical measurements were carried out using CR2025-type coin cells. Li foil was used as the counter electrode, 1 M $LiPF_6$ in a mixture of ethylene carbonate (EC), dimethyl carbonate (DMC) and ethyl methylcarbonate (EMC) (1:1:1 by volume) as the electrolyte and Celgard 2400 as the separator. The cells were assembled in a glovebox filled with highly pure argon gas (O_2 and H_2O levels less than 1 ppm) and charge/discharge tests were performed in the voltage range from 1 to 3 V (Li^+/Li) at different current rates on the LAND batteries test system (LAND CT 2001A, Wuhan, China).

Results and discussion

The spherical anatase mesocrystal was achieved by simply solvothermal treatment of HAc-TBT-BA solution together with subsequent calcination at 400 ℃ to remove the residual organics. The general morphology of as-prepared products was investigated by FESEM and TEM. The typical SEM images of anatase mesocrystals with different magnifications are displayed in **Fig.** 1(a-b). Substantially spherical products with diameters around 250-400 nm are successfully synthesized in the present reaction system. Meanwhile, their rough surfaces indicate that they are constructed by many tiny nanoparticles, which can also be demonstrated by SEM images in **Fig.** 1(b). For the detailed observation of nanoparticles, the sample was characterized by HRTEM. The arrow in **Fig.** 1(e) points out a single nanoparticle with sizes around 15 nm and the lattice fringe with spacing of 0.35 nm can be well assigned to (101) planes of anatase. The continuous and parallel lattice-fringes in the HRTEM image indicate that each attached nanoparticle shares the same crystallographic orientation. However, small lattice mismatches also exist in the boundary areas between nanoparticles for the assembly process, which can be easily observed from **Fig.** 1(e) and it is typical for mesocrystals.[6-9] Moreover, the diffraction spots of related selected area electron diffraction (SAED) pattern suggest the whole particle displays a single-crystal like structure and the nanosubunits are crystallographically oriented along [001]. Therefore, based on the results above, we can convince that spherical mesocrystals have been successfully prepared in the HAc-TBT-BA system.

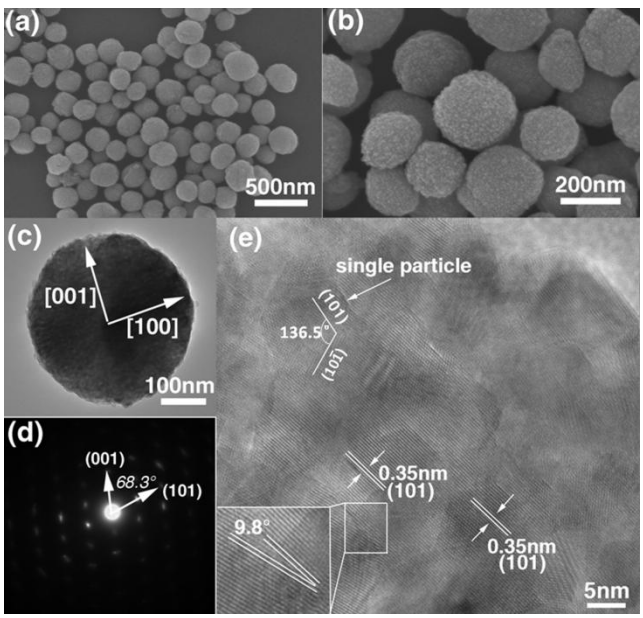

Fig. 1 (a-b) SEM images (c) TEM image (d) SAED pattern (e) HRTEM image of spherical anatase mesocrystals

Furthermore, the crystalline structure and purity of spherical mesocrystals were characterized by XRD. All the diffraction reflections displayed in **Fig.** 2(a) can be well indexed to standard anatase TiO_2 (JCPDS No. 211272). The average crystallite size based on (101) diffraction peak was calculated to be *ca.* 17.63 nm by Scherer equation, which is consistent with the observed HRTEM results. Mesocrystals usually have large surface area owing to their unique structure. Thus, the as-prepared spherical anatase mesocrystals were conducted by Brunauer-Emmett-Teller (BET) measurements to investigate their textural properties. Nitrogen adsorption-desorption isotherm of products together with the corresponding pore size distribution curve are shown in **Fig.** 2(b). The spherical anatase mesocrystals show type-IV isotherm and exhibit a broad hysteresis loop, which is characteristic of mesoporous materials. The specific surface area and pore size are 71.89 m^2/g and 5.2 nm, respectively.

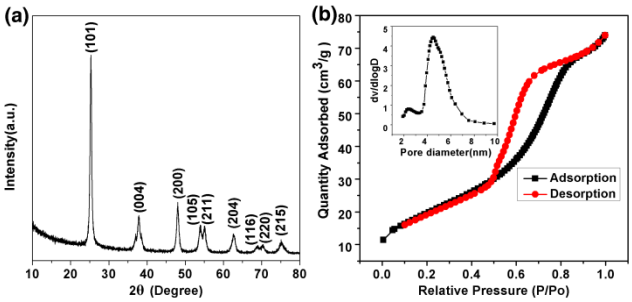

Fig. 2 (a) XRD pattern (b) N_2 adsorption-desorption isotherm of spherical anatase mesocrystals

In order to understand the formation mechanism of spherical mesocrystals, a series of time-dependent experiments were conducted. The morphology evolution under different reaction times was observed by TEM and SEM. When TBT was added into the mixture of HAc and BA, white precipitate formed immediately. According to the previous reports, the white precipitate was titanium complex (Ti-Ac and Ti-BA).[19, 35] Besides titanium complex, n-butyl alcohol formed simultaneously during the complex reaction based on the law of mass conservation, as shown in **Fig.** 3(h) Formula (1-2). With the slow increase of the reaction temperature and reaction time, further reaction of the titanium complex would be occurred. When the reaction time reached up to 1 h, some single nanorods (sizes about 0.5 μm) were obtained and flowers aggregated by these rods were also observed, which could be displayed obviously in the TEM images (**Fig.** 3(d)). As the reaction time extended to 2 hours, only flower-like products were obtained (sizes about 1 μm). The flower-like products obtained at 2 h was characterized by XRD to determine their crystalline phase. The XRD pattern reveals that the as-prepared flower-like intermediates are with an unknown crystal phase, which is similar to previous results.[19, 35] With further prolongation of reaction time, flower-like intermediates would continue to react with water which was produced during the esterification reactions between HAc, BA and n-butyl alcohol. After 5 hours, many tiny TiO_2 nanocrystals precipitated on the petals, and some nanocrystals would be self-assemblied into large nanoparticles, as shown in **Fig.** 3(f). During the generation of TiO_2 nanocrystals, esters would be formed simultaneously shown in Formula (3-4). However, esters could dissolve again in the acetic acid solution, leading to the emergence of mesoporous and disappearance of flower-like structure. Finally, spherical anatase mesocrystals were produced when the reaction time was prolonged to 24 h.

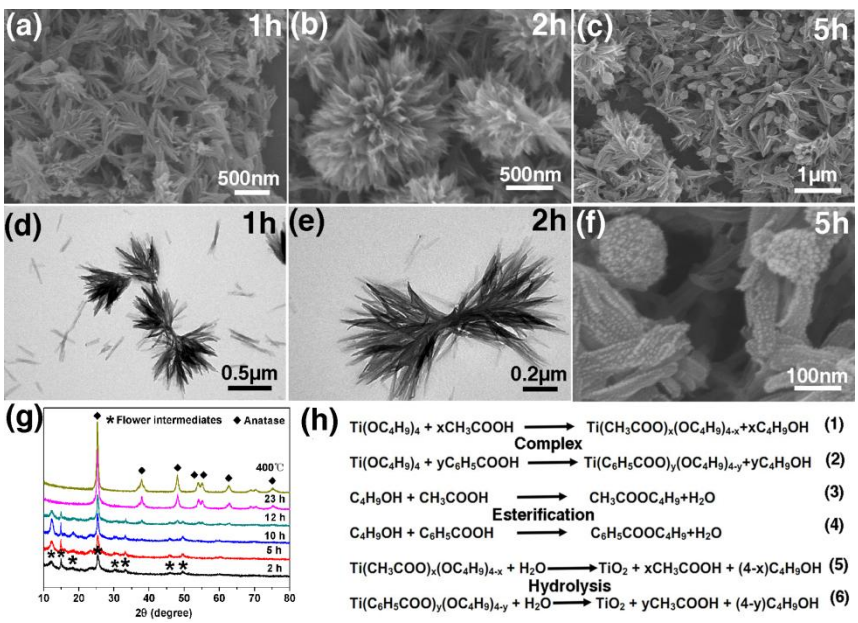

Fig. 3 (a-g) SEM, TEM images and XRD patterns of the samples obtained at 200 ℃ under 1 h, 2 h, 5 h and (h) the possible reactions in the autoclaves

According to the experimental results, a possible growth mechanism of spherical anatase mesocrystals was proposed and the corresponding schematic illustration was shown in Scheme 1. When TBT was added into the mixture solution of HAc and BA, Ti-complex would be produced firstly. With the prolongation of reaction time, Ti-complex would further react to form flower-like intermediates composed of plenty of rods. Subsequently, in the presence of water produced by esterification reaction, initial TiO_2 nanocrystals would precipitate on the petals owing to hydrolysis of the intermediates. Finally, TiO_2 nanocrystals would assemble together sharing with the same crystallographic orientation to form spherical anatase mesocrystals.

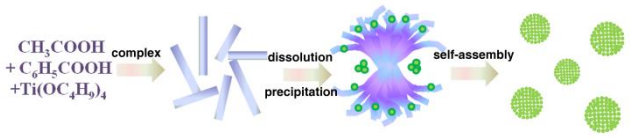

Scheme 1 Schematic illustration of formation mechanism for spherical anatase mesocrystals

In the HAc-TBT-BA reaction system, benzoic acid is the key factor to form spherical mesocrystals. To understand the effect of benzoic acid on the morphology of TiO_2 mesocrystals in-depth, contrast experiments were performed with different amounts of benzoic acid. The general morphology of products was observed by SEM and the results were shown in **Fig.** 4(a-d). Moreover, the particle diameters distribution histograms of the samples synthesized at different BA amounts and the corresponding average sizes determined by the Gaussian distribution were demonstrated in **Fig.** 5(a-c). Actually, without benzoic acid, only ellipsoidal TiO_2 were formed, which was consistent with the results of Qi.[19] When the amount of benzoic acid was very low (less than 4.5 g), part of products would turn into spheres but with a broad sizes distribution, ranging from 100 to 450 nm and giving an average size of 230 nm shown obviously in **Fig.** 5(a). As the benzoic acid additions increased to 4.5 g, only spherical products were produced with narrow sizes distribution and the average diameter was 250 nm, which was a bit larger than sample obtained at 3 g BA. However, when the amount of benzoic acid was too high, the spherical morphology of products was also maintained because of the low content of TBT. This result clearly demonstrated that the increasing amount of benzoic acid can effectively control the shape of mesocrystals from ellipsoid to sphere at a given reaction temperature and time. **Fig.** 4(e) describes the schematic illustration of ellipsoidal and spherical TiO_2. The possible role of benzoic acid in tailoring the morphology of anatase mesocrystals is reducing the growth rate of {001}. Benzoic acid is just as a protecting agent whose role is the same as 2-propanol in the synthesis of anatase TiO_2 nanosheets with dominant {001}.[36] C_6H_5COO- can selectively adsorb on {001} facet and the growth of {001} was retarded. In addition, both the steric-hinerance effect of phenyl group (C_6H_5-) and the interaction of π-π will have significant effects on the growth of nanocrystalline. The two aspects suppresses the growth rate of {001} facets synergistically, leading to the formation of spherical morphology.

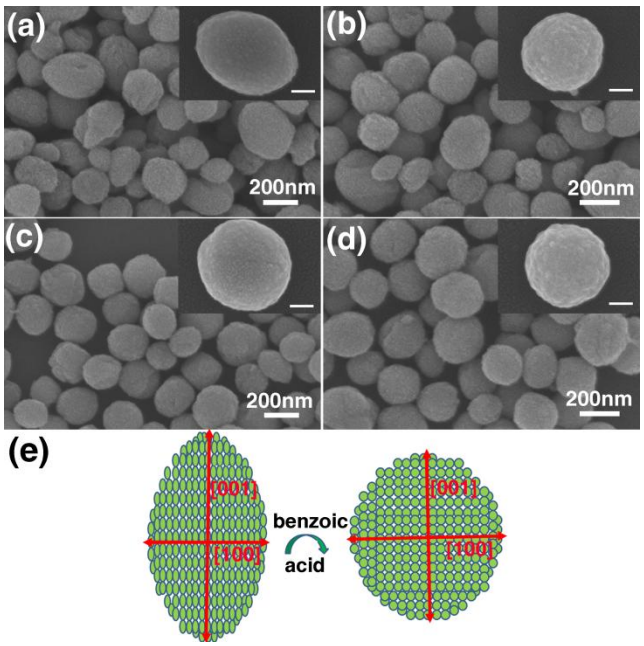

Fig. 4 SEM images of mesocrystals with different amounts of benzoic acid (a) 1.5 g (b) 3 g (c) 4.5 g (d) 9 g. The insets in (a-d) represent the high magnification SEM images of single particle (Scale bar, 100 nm) (e) Schematic illustration of ellipsoidal and spherical TiO_2

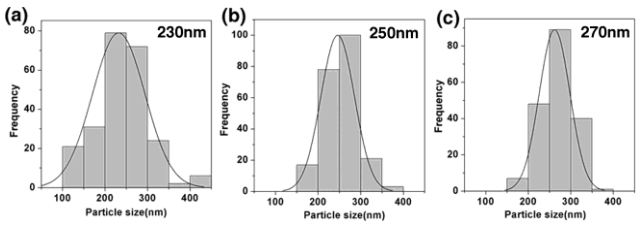

Fig. 5 Size distribution of TiO_2 mesocrystals obtained at different amounts of benzoic acid (a) 3 g (b) 4.5 g (c) 9 g

Considering the advantages of structure, the electrochemical properties of spherical anatase mesocrystals were also investigated. **Fig.** 6(a) depicts the charge-discharge voltage profiles of the TiO_2 electrode for the initial ten cycles at a current rate of 0.2 C (1 C=167.5 mAh/g) with a voltage window of 1-3 V. There are distinct potential plateaus at approximately 1.78 and 1.90 V for discharging and charging processes, corresponding to lithium-ion insertion/extraction within the anatase lattice, respectively. The first discharge and charge capacity are 314.5 224.3 mAh/g and the corresponding Coulombic efficiency is about 71.3%. In the second cycle, the discharge capacity decreases to 254.9 mAh/g with a corresponding charge capacity of 213.4 mAh/g, leading to a higher Coulombic efficiency of 83.7%. After 10 cycles, the capacity is retained at 200 mAh/g, and the Coulombic efficiency is up to 100%, indicating a good cycling stability.

Cycling and rate performances are two critical indicators of Li-ion batteries. **Fig.** 6(b) shows the cycling performance of spherical anatase mesocrystals at different current rates of 1 C, 2 C and 5 C. The initial discharge capacities are 239.9, 187.1 and 160.2 mAh/g, respectively. After 50 cycles, the spherical anatase

mesocrystals achieved capacity retentions of 160 mAh/g when cycled at 1 C, which is about 95% of practical capacity (167.5 mAh/g). Even cycling at high current densities, such as 2 C and 5 C, these spherical anatase mesocrystals remain high capacity and well stability, *e.g.* the capacity retains 120 and 115 mAh/g at a current rate of 2 C and 5 C after 50 cycles. Contrast with some previous reports, the nanocrystalline TiO_2 mesoporous microspheres electrode (TiO_2 sphere/conductive agent/binder = 85:10:5) [28] and TiO_2 electrode (TiO_2/conductive agent/binder = 80:10:10) [37] showed discharge capacities of 120, and 90 mAh/g at 1.2 and 0.25 C rate, respectively. The good cycling performance of spherical anatase mesocrystal is ascribed to the short transport distance of Li^+, fast electron transport rate, large specific surface area and stable structure of spherical anatase mesocrystals. The rate performance of TiO_2 from 0.2 C to 2 C for 10 cycles is displayed in **Fig.** 6(c). After an initial discharge capacity of 320 mAh/g, the capacity was found to stabilize at 195 mAh/g at 0.2 C. Further cycling at 0.5, 1 and 2 C, the spherical anatase mesocrystals showed high reversible capacities of 170, 150 and 120 mAh/g, respectively. When the C-rate was switched from 2 C to 0.5 C again, the original capacity was largely recovered, indicating the stability of the electrode materials. The good rate performance is due to its high crystallinity, mesoporous structure and small primary particle size. All these indicated that, spherical anatase mesocrystal will be a very promising anode.

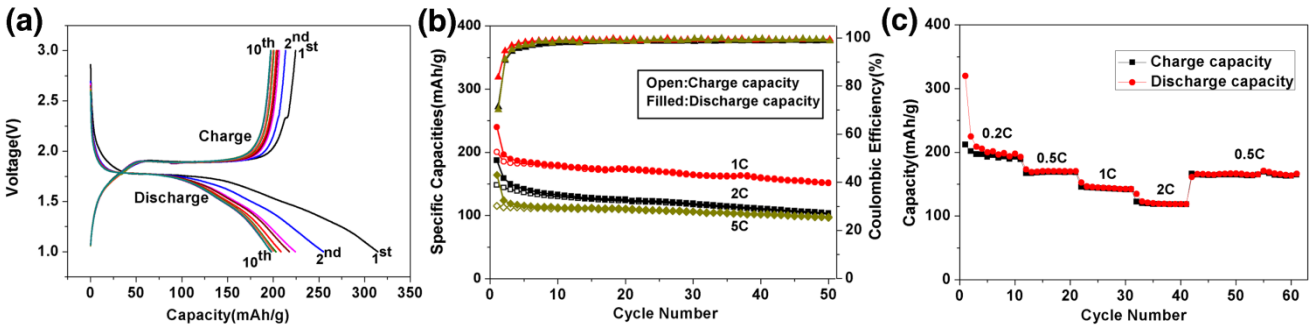

Fig. 6 (a) The initial ten discharge/charge voltage profiles of spherical mesocrystals at 0.2 C with a voltage window of 1-3 V (b) Cycling performance of TiO_2 mesocrystals at current rates of 1 C, 2 C and 5 C (c) Rate performance of TiO_2 from C/5 to 2 C (1 C=167.5 mAh/g) for ten cycles

Conclusions

In conclusion, spherical anatase mesocrystals were successfully prepared in HAc-TBT-BA system. They possess high crystallinity and large specific surface area simultaneously. The formation process of mesocrystals mainly contains the formation of titanium complex, generation of flower-like intermediates, slow hydrolysis of intermediates, precipitation and self-assembly of initial anatase nanocrystals. Benzoic acid is the key factor to form spherical morphology and increasing the amount of benzoic acid can effectively change the shape of mesocrystals from ellipsoid to sphere. These spherical anatase mesocrystals exhibit high reversible capacities and good rate performance when used as anode materials. It has given us a signal that spherical anatase mesocrystals will be great potential anode materials in the near future.

Acknowledgements

The authors gratefully acknowledge the financial support for this work from the Doctoral Fund of the Ministry of Education of China (No. 20100101110039).

Notes and references

[a] *State Key Laboratory of Silicon Materials, Department of Materials Science and Engineering, Zhejiang University, Hangzhou, China. Fax: 86 0571 87952334; Tel: 86 0571 87952334; E-mail: wangzhiyu@zju.edu.cn*

1 A. Imhof and D. J. Pine, *Nature*, 1997, **389**, 948-951.
2 Z. Y. Yuan and B. L. Su, *Journal of Materials Chemistry*, 2006, **16**, 663-677.
3 M. Li, H. Schnablegger and S. Mann, *Nature*, 1999, **402**, 393-395.
4 X. C. Wang, J. C. Yu, C. M. Ho, Y. D. Hou and X. Z. Fu, *Langmuir*, 2005, **21**, 2552-2559.
5 L. Shen, C. Yuan, H. Luo, X. Zhang, K. Xu and Y. Xia, *Journal of Materials Chemistry*, 2010, **20**, 6998-7004.
6 H. Cölfen and M. Antonietti, *Angewandte Chemie-International Edition*, 2005, **44**, 5576-5591.
7 R. Q. Song and H. Cölfen, *Advanced Materials*, 2010, **22**, 1301-1330.
8 L. Zhou and P. O'Brien, *Small*, 2008, **4**, 1566-1574.
9 L. Zhou and P. O'Brien, *Journal of Physical Chemistry Letters*, 2012, **3**, 620-628.
10 D. Zhang, G. Li, F. Wang and J. C. Yu, *CrystEngComm* 2010, **12**,1759-1763.
11 P. Tartaj, *Chemical Communications*. 2011, **47**, 256-258.
12 I. Bilecka, A. Hintennach, I. Djerdj, P. Novak and M. Niederberger, *Journal of Materials Chemistry*, 2009, **19**, 5125-5128.
13 M. S. Mo, S. H. Lim, Y. W. Mai, R. K. Zheng and S. P. Ringer, *Advanced Materials*, 2008, **20**, 339-+.
14 X. Lu, X. Li, F. Chen, C. Ni and Z. Chen, *Journal of Alloys and Compounds*, 2009, **476**, 958-962.
15 J. Ma, J. Teo, L. Mei, Z. Zhong, Q. Li, T. Wang, X. Duan, J. Lian and W. Zheng, *Journal of Materials Chemistry*, 2012, **22**, 11694-11700.
16 L. Zhou, D. S. Boyle and P. O'Brien, *Chemical Communications*, 2007, 144-146.
17 L. Zhou, D. Smyth-Boyle and P. O'Brien, *Journal of the American Chemical Society*, 2008, **130**, 1309-1320.
18 L. Li and C.Y. Liu, *Crystengcomm*, 2010, **12**, 2073-2078.
19 J. Ye, W. Liu, J. Cai, S. Chen, X. Zhao, H. Zhou and L. Qi, *Journal of the American Chemical Society*, 2011, **133**, 933-940.
20 Z. Hong, M. Wei, T. Lan, L. Jiang and G. Cao, *Energy & Environmental Science*, 2012, **5**, 5408-5413.
21 P. Tartaj and J. M. Amarilla, *Advanced Materials*, 2011, **23**, 4904-4907.
22 C. J. Barbe, F. Arendse, P. Comte, M. Jirousek, F. Lenzmann, V. Shklover and M. Gratzel, *Journal of the American Ceramic Society*, 1997, **80**, 3157-3171.
23 X. He, C. Hu, B. Feng, B. Wan and Y. Tian, *Journal of the Electrochemical Society*, 2010, **157**, J381-J385.

24 M. Ye, J. Gong, Y. Lai, C. Lin and Z. Lin, *Journal of the American Chemical Society*, 2012, **134**, 15720-15723.
25 R. Q. Song and H. Cölfen, *Crystengcomm*, 2011, **13**, 1249-1276.
26 F. Zhang, Y. Zhang, S. Song and H. Zhang, *Journal of Power Sources*, 2011, **196**, 8618-8624.
27 Y. M. Jiang, K. X. Wang, X. X. Guo, X. Wei, J. F. Wang and J. S. Chen, *Journal of Power Sources*, 2012, **214**, 298-302.
28 J. Wang, Y. Zhou, Y. Hu, R. O'Hayre and Z. Shao, *Journal of Physical Chemistry C*, 2011, **115**, 2529-2536.
29 G. Sudant, E. Baudrin, D. Larcher and J.-M. Tarascon, *Journal of Materials Chemistry*, 2005, **15**, 1263-1269.
30 M. Wagemaker, W. J. Borghols and F. M. Mulder, *Journal of the American Chemical Society*, 2007, **129**, 4323-4327.
31 D. Bresser, E. Paillard, E. Binetti, S. Krueger, M. Striccoli, M. Winter and S. Passerini, *Journal of Power Sources*, 2012, **206**, 301-309.
32 D. Bresser, B. Oschmann, M. N. Tahir, W. Tremel, R. Zentel and S. Passerini, *Journal of Power Sources*, 2014, **248**, 852-860.
33 B. Huang, X. Zheng, D. Jia and M. Lu, *Electrochimica Acta*, 2010, **55**, 1227-1231.
34 S. K. Das, S. Darmakolla and A. J. Bhattacharyya, *Journal of Materials Chemistry*, 2010, **20**, 1600-1606.
35 J. Y. Liao, B. X. Lei, D. B. Kuang and C. Y. Su, *Energy & Environmental Science*, 2011, **4**, 4079-4085.
36 H. G. Yang, G. Liu, S. Z. Qiao, C. H. Sun, Y. G. Jin, S. C. Smith, J. Zou, H. M. Cheng and G. Q. Lu, *Journal of the American Chemical Society*, 2009, **131**, 4078-4083.
37 L. J. Fu, H. Liu, H. P. Zhang, C. Li, T. Zhang, Y. P. Wu and H. Q. Wu, *Journal of Power Sources*, 2006, **159**, 219-222.